

# Analysis of formability of AISI 304 steel sheets with different thicknesses by the tensile properties

## Análisis de la formabilidad de láminas de acero AISI 304 con diferentes espesores mediante sus propiedades de tracción

Jhon Barbosa-Jaimes <sup>1a</sup>, Ismael García-Páez <sup>1b</sup>, Victoriano García-Medina <sup>2</sup>

<sup>1</sup>Grupo de investigación Gestindustriales-EOCA, Escuela de Ciencias Básicas, Tecnología e Ingeniería ECBTI, Universidad Nacional Abierta y a Distancia UNAD, Colombia. Orcid: 0000-0001-7890-2678 <sup>a</sup>, 0000-0003-0698-6395 <sup>b</sup>. Emails: [jhon.barbosa@unad.edu.co](mailto:jhon.barbosa@unad.edu.co) <sup>a</sup>, [victoriano.garcia@unad.edu.co](mailto:victoriano.garcia@unad.edu.co) <sup>b</sup>

<sup>2</sup>Grupo de investigación en Diseño Mecánico, Materiales y Procesos-GIDIMA, Departamento de Diseño Mecánico Materiales y procesos, Universidad Francisco de Paula Santander UFPS, Colombia. Orcid: 0000-0002-2590-5661. Email: [ismaelhumbertogp@ufps.edu.co](mailto:ismaelhumbertogp@ufps.edu.co)

Received: 25 May 2022. Accepted: 23 June 2022. Final version: 30 October 2022.

### Abstract

Although AISI 304 steel is widely used and its manufacturers provide resistance data in the quality certificate, these are not sufficient to characterize and predict the behavior of the sheets in the drawing and drawing processes. This is why the objective of this work was to analyze the formability of AISI 304 steel sheets with 16- (thickness 1.5 mm), 18- (1.2 mm), and 20- (0.9 mm) gauges used by the metalworking industry in Colombia by determining intrinsic properties related to the ability of the sheet to withstand stretching and drawing operations such as the strain hardening exponent  $n$ , the normal anisotropy  $r_m$ , and the planar anisotropy  $\Delta r$ . The methodology consisted of analyzing the chemical composition, a metallographic study, and a series of tensile tests. The results show that the steel has a microstructure of twinned austenite grains of size between 15-30  $\mu\text{m}$ . Regarding the mechanical resistance, it was observed that all the mean values of ultimate resistance, elastic limit, and elongation are above the minimum established in the standard. Furthermore, all of the tensile test results changed according to the variation of angles concerning the rolling direction ( $0^\circ$ ,  $45^\circ$ , and  $90^\circ$ ), which indicates the anisotropic character of the sheet. The most relevant result allows us to infer that the 20-gauge sheet has better formability and therefore, better behavior against the stretching and drawing processes.

**Keywords:** Anisotropy; Formability; Metallic sheet; Mechanical properties; AISI 304L; Deep drawing; Stretched; Metalworking industry; Microstructure; Grain size.

### Resumen

Aunque el AISI 304 es ampliamente utilizado y sus fabricantes suministran en el certificado de calidad datos de resistencia, estos no son suficientes para caracterizar y predecir el comportamiento de las láminas en los procesos de estirado y embutido. Es por esto que el objetivo de este trabajo fue el de analizar la formabilidad de láminas de Acero AISI 304 con calibre 16 (espesor 1.5 mm), 18 (1,2 mm) y 20 (0.9 mm) utilizados por la industria metalmeccánica en

ISSN Printed: 1657 - 4583, ISSN Online: 2145 - 8456.

This work is licensed under a Creative Commons Attribution-NoDerivatives 4.0 License. [CC BY-ND 4.0](https://creativecommons.org/licenses/by-nd/4.0/)



How to cite: J. Barbosa-Jaimes, I. García-Páez, V. García-Medina, "Analysis of formability of AISI 304 steel sheets with different thicknesses by the tensile properties," *Rev. UIS Ing.*, vol. 21, no. 4, pp. 97-106, 2022, doi: <https://doi.org/10.18273/revuin.v21n4-2022009>

Colombia mediante la determinación de propiedades intrínsecas relacionadas con la capacidad de la lámina para soportar operaciones de estirado y embutido tales como: el exponente de endurecimiento por deformación  $n$ , la anisotropía normal  $r_m$  y de la anisotropía planar  $\Delta r$ . La metodología consistió en realizar un análisis de la composición química, un estudio metalográfico, y una serie de ensayos de tracción basados en las normas ASTM. Los resultados muestran que el acero puede clasificarse del grado 304L, con una microestructura conformada, para los tres espesores, por granos equiaxiales de austenita de tamaño entre 15-30  $\mu\text{m}$  con presencia de maclas. En cuanto a la resistencia mecánica se pudo observar que todos los valores promedio de resistencia última, límite elástico y alargamiento están por encima de los mínimos establecidos en la norma. Además, todos los resultados de la prueba de tracción cambian de acuerdo al ángulo de maquinado de la probeta respecto a la dirección de laminación ( $0^\circ$ ,  $45^\circ$  y  $90^\circ$ ), lo que indica el carácter anisotrópico de la lámina. Los resultados más relevantes permiten inferir que la lámina calibre 20 tiene mejor formabilidad y, por ende, mejor comportamiento frente a los procesos de estirado y embutido.

**Palabras clave:** anisotropía; formabilidad; lámina metálica; propiedades mecánicas; AISI 304L; embutido profundo; estirado; industria metalmeccánica; microestructura; tamaño de grano.

## 1. Introduction

Sheet metal forming is the process by which a flat sheet of metal is transformed into another shape without failure, fracture, or excessive thinning. The process can be simple, for example, a bending, or a very complex sequence of operations to produce high volumes of parts by stamping [1]. Forming operations are so diverse in type, magnitude, and speed that no single test accurately indicates a material's formability in all situations. However, the knowledge of the material's properties and the detailed analysis of the type of operation used are essential in the manufacture of a specific piece and the development of the most efficient process [1].

Formability refers to the amount of deformation that can be obtained from sheet metal in a manufacturing process before failure [2], [3]. This property depends on several factors such as thickness, manufacturing process, speed, lubrication, and, to a large extent, the intrinsic properties of the material [4], [5].

The tests used to predict the formability of metal sheets are divided into two: First, the intrinsic test for determining specific information on the material does not consider the conditions of the sheet, such as thickness [5], the standard tensile test [6], and the second is simulations test that provides specific but limited information on the manufacturing process and its operating conditions [7], such as the test to determine the formability limit curve (FLC), which provides the maximum deformation delivered by a shell before failure occurs [2], [8].

From the mechanical properties resulting from the tensile test (intrinsic), which can be related to the formability of the sheet, the following are found the elongation at break, A50, indicates the ductility of the material, which is why it is related to the forming capacity of the metal sheet [3], [4], [9].

The strain hardening exponent,  $n$ , indicates how quickly the sheet increases the strength and hardness due to plastic deformation [5]. Its elongation is more significant in a sheet with a high value of the exponent,  $n$ , and subjected to drawing operations. Its thickness decreases more uniformly before necking or failure appears. This behavior is an indicator of good formability [10], [11], [4]. The above also reveals a large difference between yield stress and the ultimate strength of a material [1].

Finally, the anisotropy coefficient,  $r$ , measures the quality of a material to assume different properties in different directions. For example, according to ASTM E517 [12], in metal sheets, the anisotropy coefficient  $r$  is a parameter that indicates the ability of a sheet to resist thinning or thickening when subjected to traction or compression forces in the plane of the sheet. For Gedney [5], the value of  $r$  is considered a measure of the drawing capacity of the sheet.

According to Kalpakjian and Schmid [11], this capacity is acquired in the sheet formation process. It is given by the preferential orientation of the grains and the alignment of impurities and inclusions throughout the thickness (mechanical fiberization).

For Güemes and Martin [13], the higher the anisotropy normal is, the better the material's behavior. Since if it is small, cracks or tears may appear in the process of obtaining parts by drawing. In the case of planar anisotropy, it is preferred that  $\Delta r = 0$ , because if  $\Delta r$  is large, the sheet deforms more in some directions than in others, and the problem of ear formation occurs in the drawing process, in addition to a variation in the thickness of the walls of the piece in different parts.

In this work, the mechanical characterization of AISI 304 steel sheets was carried out using tensile tests. Parameters that are not normally supplied by manufacturers, but that are required by the metalworking industry for the

continuous improvement of the productivity and quality of the products obtained in processes such as drawing and drawing of stainless steel sheets, were determined.

## 2. Materials and methods

For this investigation, AISI 304 steel sheets with 16- (1.5 mm), 18- (1.2 mm), and 20- (0.9 mm) gauges were selected, which are the most commercially used. The necessary specimens were machined from these sheets to perform the elemental chemical analysis, the metallographic study, and the tensile tests according to the ASTM standards.

The chemical analysis was performed in a BRUKER Optical Emission Spectrometer (OES), model Q8 MAGELLAN, and BAS No. 467/1 was used as reference material.

Metallographic preparation was performed using a standard procedure: mounting the test piece in Bakelite, grinding with SiC papers up to 1000 grit, and polishing with 0.5-micron aluminum oxide. The microstructure was revealed by etching with hydrochloric acid and hydrogen peroxide (100 mL water, 300 mL of HCl, 15 mL of 30% hydrogen peroxide) solution freshly prepared.

For the tensile test, samples at 0°, 45°, and 90° concerning the last lamination were cut in a CNC machining center, with the water jet method, as shown in [Figure 1](#).

The tensile test was performed in a SHIMADZU universal traction/compression testing machine, model Autograph AG-X plus, with a 100 KN load cell and an Epsilon extensometer up to 20% deformation. With the data obtained in this test, the conventional elastic limit ( $\sigma_y$ ), tensile strength ( $\sigma_u$ ), elongation at break (A50), and the strain hardening exponent ( $n$ ) were calculated.

Four samples were tested for each orientation (12 for each sheet thickness). The test speed was set at 1 mm/min before the elastic limit and 5 mm/min after the elastic limit and before the ultimate stress. Both, the measurements of the specimen and the speed conditions of the test are under the provisions of the standards ASTM E 8M and ASTM E 646 [6], [14].

After each test, the results of the tensile strength ( $\sigma_u$ ) and the conventional elastic limit by the creep method (offset 0.2%) ( $\sigma_y$ ) are obtained directly from the universal machine software. The final gauge length is measured and the percent elongation at break (A50) is calculated.

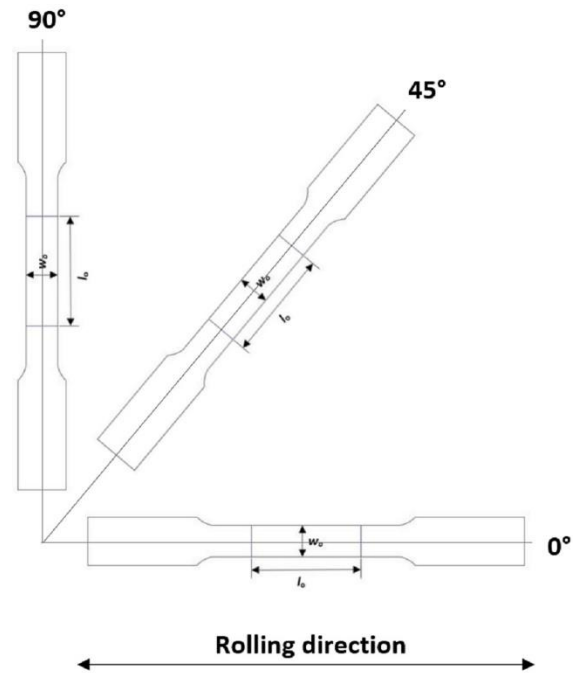


Figure 1. Arrangement of machined samples with orientations of 0°, 90°, and 45° to the direction of the last rolling. Source: authors.

The logarithmic representation of the results of the true stress vs. the true strain allows for determining the value of the strain hardening exponent ( $n$ ) using the empirical mathematical Equation (1), which applies to metallic materials [14].

$$\sigma_r = k * \epsilon^n \quad (1)$$

$\sigma_r$  = true stress.

$\epsilon$  = true strain.

$k$  = strength coefficient.

$n$  = strain-hardening exponent.

The values of real stress  $\sigma_r$  and real strain  $\epsilon$  were calculated from the data of stress  $\sigma$  and engineering strain  $\epsilon_e$ , obtained in the tensile test as shown in Equation (2) and Equation (3):

$$\sigma_r = \sigma * (1 + \epsilon_e) \quad (2)$$

$$\epsilon = \ln(1 + \epsilon_e) \quad (3)$$

Equation (1) written in logarithmic form, equation (4), indicates that the points must be plotted on a logarithmic scale, or plot directly the logarithms of the values obtained, as shown in [Figure 2](#).

$$\log \sigma_r = \log k + n \log \epsilon \quad (4)$$

Using linear regression by the least-squares numerical method with the pairs of points ( $\sigma$ ,  $\epsilon$ ) the value of the strain hardening exponent  $n$  is obtained, as indicated by the standard [14].

The data used in the calculation, strains between 10 and 20%, correspond to the range between the elastic limit and before the necking begins at the ultimate engineering stress point [14], the range over which the equations for calculating actual stresses and strains are applicable [15].

Since in all cases the elastic deformation is considerably less than 10% of the real total deformation, this can be considered negligible, as suggested by [15], therefore, method B of the ASTM E 646 standard was applied [14].

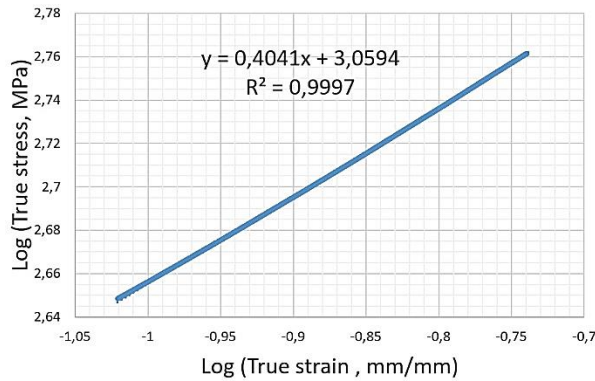


Figure 2. Log-log true stress–true strain diagram, between the elastic limit and the maximum stress.  
Source: authors.

The anisotropy coefficient ( $r$ ) was determined in an IBERTEST universal traction/compression machine, model IBMT2-600. The test was realized to 5 samples for each orientation (15 for each sheet thickness), the strain rate was set at 4 mm/min, and the measurements were carried out under the ASTM E 517 standard [12]. The test ended when the length deformation in the original calibrated zone reached 20%, ( $l_f = 60$  mm) Figure 3.

The initial and final distances in the samples were measured. Then, the anisotropy coefficient was calculated for each specimen (1, 2, 3, 4, and 5) in the three directions ( $0^\circ$ ,  $45^\circ$ ,  $90^\circ$ ) of the three thicknesses (0.9, 1.2, and 1.5 mm) using Equation (5):

$$r = \frac{\epsilon_w}{\epsilon_t} = \frac{\ln\left(\frac{w_o}{w_f}\right)}{\ln\left(\frac{l_f * w_f}{l_o * w_o}\right)} \quad (5)$$

$\epsilon_w =$  width strain.

$\epsilon_t =$  thickness strain.

$l_o =$  original gauge length.

$l_f =$  final gauge length.

$w_o =$  original width.

$w_f =$  final width.

The results of the 5 samples were averaged and the values of  $r$  in each direction were obtained:  $r_0$ ,  $r_{45}$  y  $r_{90}$ , for each thickness.

Finally, normal anisotropy and planar anisotropy were calculated for each shell thickness, using Equation (6) and Equation (7), respectively [16].

$$r = \frac{r_0 + 2r_{45} + r_{90}}{4} \quad (6)$$

$$\Delta r = \frac{r_0 - 2r_{45} + r_{90}}{2} \quad (7)$$

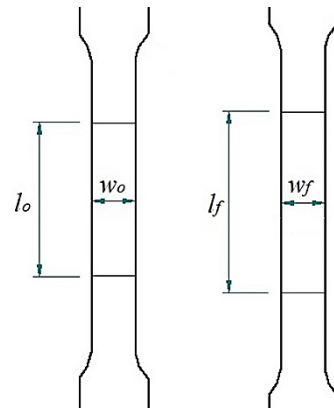


Figure 3. Measurements for determining  $r$ -values.  
Source: authors.

### 3. Results and discussion

The elemental chemical analysis presented in Table 1 confirms that the material studied is 304 Steel, which can be classified as 304L grade, due to its low carbon content, 0.028%, 0.020%, and 0.025%. This grade of steel is often preferred in applications where welding is required as it eliminates the formation of chromium carbides during cooling in the heat-affected zone, HAZ [17].

Figure 4 shows the microphotograph of the 18-gauge sample. In general, there are no significant differences between the microstructures of the three-gauge samples, and it comprises nearly equiaxed polygonal grains with annealing twins. The grain size of the austenite is between 10 and 25  $\mu\text{m}$ . Since no alignment of the grains is observed in the direction of the last rolling, it is considered that the sheets were subjected to an adequate

annealing process. Therefore, a marked anisotropic behavior is not expected.

Table 1. Chemical analysis of the steels under study measured by EOS

Element	Gauge 16 1.5 mm wt. %	Gauge 18 1.2 mm wt. %	Gauge 20 0.9 mm wt. %
(C)	0.028	0.020	0.025
(Si)	0.464	0.506	0.438
(Mn)	1.476	1.315	1.630
(P)	0.029	0.029	0.036
(S)	0.0054	0.0054	0.0054
(Cr)	18.24	18.12	18.13
(Mn)	0.064	0.014	0.430
(Ni)	8.120	8.131	8.1
(Cu)	0.031	0.027	0.490
(Al)	<0.00050	<0.00050	<0.00050
(As)	0.0075	0.0067	0.010
(B)	0.00022	0.0011	0.00031
(Co)	0.203	0.253	0.230
(Nb)	0.0066	0.0046	0.021
(Pb)	0.0042	0.0036	0.0043
(Sn)	0.00054	<0.00050	0.0097
(Ti)	0.0085	0.0080	0.0081
(V)	0.170	0.137	0.144
(W)	<0.0020	<0.0020	0.055

Source: authors.

The grain size considerably affects the properties of the material [18], the fine grain is associated with greater strength and hardness, but less ductility, and the coarse grain with greater roughness in the appearance of the surface "orange peel" [11]. The value between 10 and 25  $\mu\text{m}$  is close to the ASTM grain size 7 suggested for sheet metal forming operations [11].

In Table 2, the results of the conventional elastic limit of 0.2% ( $\sigma_{y 0.2\%}$ ) and the tensile strength ( $\sigma_u$ ) for sheet thickness according to its orientation. The mean values of the tensile strength of the 16-, 18- and 20-gauge sheets are 666.133, 600.631, and 530.220 MPa, respectively.

Regarding the conventional elastic limit of 0.2%,  $\sigma_y$  (0.2%), the resistance values for the 16-, 18- and 20-gauge sheets are 286.015, 251.160, and 253.273 MPa, respectively.

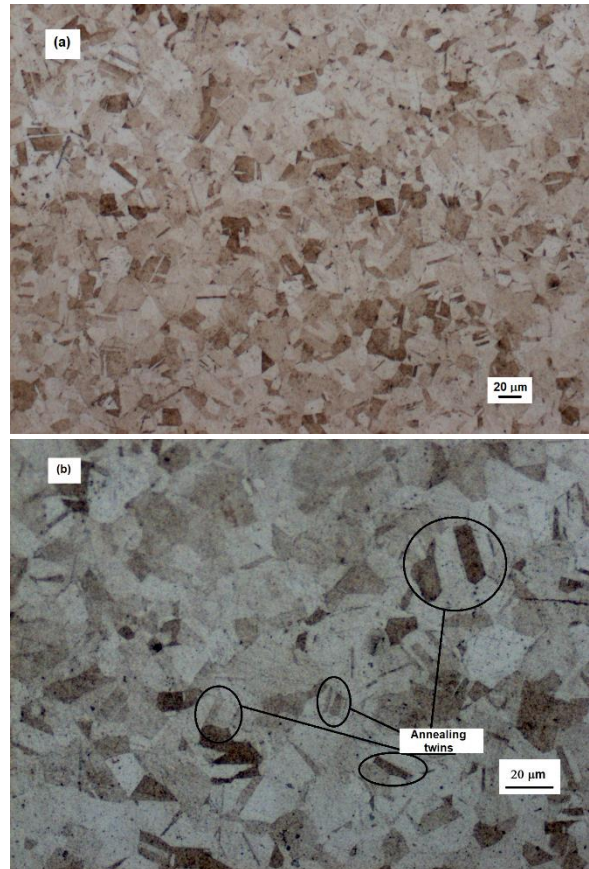


Figure 4. Microstructure of the 18-gauge sample. (a) low magnification, (b) high magnification. They were etched with HCl and H<sub>2</sub>O<sub>2</sub> by 3 s. Source: authors.

Figure 5 shows a comparison of the engineering curves of the 16-, 18-, and 20-gauge sheets for the 0° orientation. 16-gauge sheets have higher strength, while 18- and 20-gauge sheets do not differ significantly from each other. This behavior is observed in all three orientations. As mentioned above, in all cases the elastic deformation is considerably less than 10% of the real total deformation, therefore, method B of the ASTM E 646 standard was applied.

The mean values of the tensile strength and the conventional elastic limit of the studied steel are very similar to those reported by [19] for an AISI 304 DDQ steel (drawing quality) of 0.8 mm thickness: 582 and 252 MPa, respectively. In turn, they are slightly lower than those reported by [20] for an AISI 304 steel with a thickness of 0.7 mm: 662 and 284 MPa, respectively, as well as those written by [21] for an AISI 304L steel with a thickness of 1,168 mm: 670.4 and 290.8 MPa.

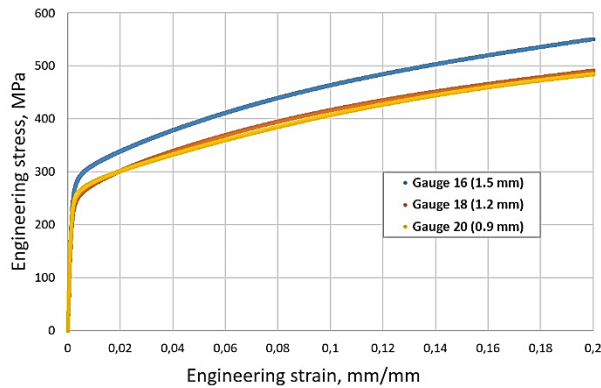


Figure 5. Comparative curves engineering stress vs engineering strain of AISI 304 steel sheets for 16-, 18- and 20-gauge for the 0° orientation. Source: authors.

Table 2. Elastic limit and tensile strength for the three sheet thicknesses

Gauge		Tensile strength ( $\sigma_u$ ) Mpa	Yield strength ( $\sigma_y$ ) Mpa
16 (1.5 mm)	0°	687.179 ± 5.482	287.297 ± 5.867
	45°	647.428 ± 13.690	279.762 ± 5.361
	90°	663.791 ± 6.257	290.986 ± 5.441
18 (1.2 mm)	0°	614.412 ± 1.636	248.017 ± 3.321
	45°	588.243 ± 2.845	252.511 ± 4.167
	90°	599.238 ± 2.100	252.954 ± 0.763
20 (0.9 mm)	0°	549.487 ± 9.970	255.112 ± 2.120
	45°	515.401 ± 5.910	251.563 ± 6.251
	90°	525.772 ± 9.329	253.146 ± 7.672
304 ASTM A 240		515	205
304 ASTM A 240		485	170

Source: authors.

The values of elongation at break in 50mm of calibrated length (A50) obtained in the tensile test for each sheet thickness according to orientation are shown in Table 3. The mean values for the 16-, 18- and 20-gauge sheets are 57.38, 58.45, and 63.32% respectively. These values are very similar to the 57% reported by [20] for an AISI 304 steel with a thickness of 0.7 mm, and the 64% reported by [21] for an AISI 304L steel with a thickness of 1.168 mm.

Although according to what was observed in the microstructure, an anisotropic behavior was not expected, an elongation lower. Therefore, lower ductility was observed in the direction of the last lamination (0°) to the other orientations in all three gauges.

Table 3. Elongation at break for the three sheet thicknesses

Gauge		Percent elongation in 50 mm ( $A_{50}$ ) %
16 (1.5 mm)	0°	53.93 ± 1.09
	45°	58.26 ± 0.32
	90°	59.96 ± 1.25
18 (1.2 mm)	0°	56.14 ± 1.12
	45°	60.03 ± 2.02
	90°	59.19 ± 1.41
20 (0.9 mm)	0°	59.22 ± 1.33
	45°	64.83 ± 1.35
	90°	65.91 ± 1.99
304 ASTM A 240		40
304L ASTM A 240		40

Source: authors.

The strength and elongation values determined in this study are above the minimum values established for AISI 304 and AISI 304L steel sheets according to the ASTM A 240 standard [22].

The results obtained from the strain hardening exponent ( $n$ ) for the steels studied according to their thickness and their orientation are shown in Table 4. Again, a behavior similar to that of the elongation is observed, in which the value in the direction of the last lamination is different, in this case, higher than those of the other orientations, indicating a slight anisotropic behavior, especially in the 18- and 20-gauge sheets, as can be seen in Figure 6.

The results are very similar, both for the three thicknesses and for the three orientations. The values (mean) were 0.378, 0.371, and 0.393 for 16-, 18- and 20-gauge sheets, respectively, which are higher than the 0.244 reported by [19] for a 0.8 mm thickness AISI 304 DDQ (drawing quality) steel. However, they are slightly lower than the 0.42 reported by [20] for a 0.7 mm thickness AISI 304 steel, and the 0.52 written by [21] for a 1.168 mm thickness AISI 304L steel.

Table 5 shows the results of the anisotropy coefficient,  $r$  for each sheet according to their orientations concerning the rolling direction and the influence of the normal and planar anisotropy for each thickness.

Table 4. Values of the strain hardening exponent for the three sheet thicknesses

Gauge		Strain-Hardening Exponents, $n$
16 (1,5 mm)	0°	$0.381 \pm 0.005$
	45°	$0.379 \pm 0.003$
	90°	$0.376 \pm 0.002$
18 (1,2 mm)	0°	$0.388 \pm 0.002$
	45°	$0.360 \pm 0.001$
	90°	$0.363 \pm 0.002$
20 (0,9 mm)	0°	$0.409 \pm 0.010$
	45°	$0.382 \pm 0.004$
	90°	$0.390 \pm 0.005$

Source: authors.

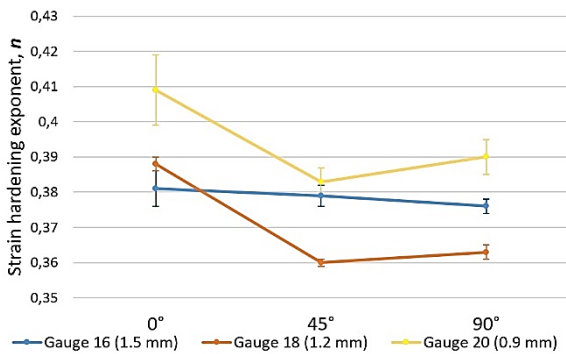


Figure 6. Comparative diagram between values of the strain hardening exponent in AISI 304 steel sheets for 16-, 18- and 20-gauge. Source: authors.

Figure 7 shows the average value of 5 samples for each orientation of the sheets of the three gauges. It can be seen that the greater the thickness of the sheet, the greater the value of  $r$  in its three directions. The highest values were observed for 45° samples, marking more difference in caliber 16. Although there is no marked dispersion in the data, some authors associate this with the crystallographic texture of the material [9], [23].

Values of the normal anisotropy,  $r_m$ , determined by Equation (6): 1.05; 0.99, and 0.93 are slightly higher than the 0.906 obtained by Coello and others for an AISI 304 steel (drawing quality) of 0.8 mm thickness [19]. Similarly, they are less than the 2.44 reported by du Toit and Steyn for a 0.7 mm thickness AISI 304 steel [20], and similar to the  $r_0=1,01$   $r_{90}=0,91$  written by V. Talyan for a steel AISI 304L 1,168mm thickness [21].

Table 5. Anisotropy coefficient for the three sheet thicknesses

Gauge	Plastic strain ratio, $r$ Equation (5)	Normal anisotropy Equation (6)	Planar anisotropy Equation (7)
		$r_m$	$\Delta r$
16 (1.5 mm)	$r_0$	1.05	-0.19
	$r_{45}$		
	$r_{90}$		
18 (1.2 mm)	$r_0$	0.99	-0.15
	$r_{45}$		
	$r_{90}$		
20 (0.9 mm)	$r_0$	0.93	-0.11
	$r_{45}$		
	$r_{90}$		

Source: authors.

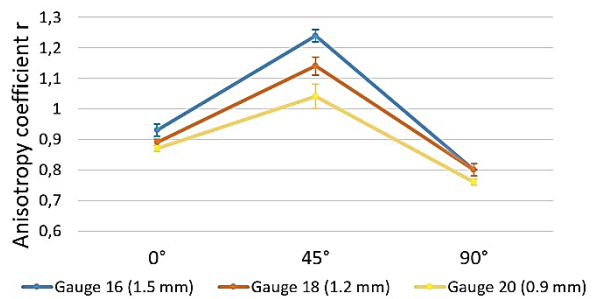


Figure 7. Comparative diagram between mean values of the anisotropy coefficient  $r$  (equation 5) in the steel sheets for the AISI 304 20-, 18- and 16-gauge. Source: authors.

Regarding the results of the planar anisotropy,  $\Delta r$ , calculated using Equation (7), the values of -0.19; -0.15, and -0.11 are closer to zero than the -0.22 published by du Toit and Steyn for 0.7 mm thickness AISI 304 steel [20]. This behavior indicates that the sheets object of this study would be less susceptible to the formation of ears in the drawing process.

#### 4. Conclusions

The elemental chemical composition allows classifying the steels used in the study as AISI 304 grade L because their carbon content is less than 0.03%.

The metallographic study shows austenite as the only phase, in the form of twinned equiaxed grains with sizes between 4 and 5 ASTM.

These results indicate that an annealing process eliminated grain deformation along the last rolling direction, but increased grain size, especially for use in the drawing process.

The mean values of resistance to traction, of the conventional elastic limit of 0.2%,  $\sigma_y$ , (0.2%), and of the normal and planar anisotropy coefficient show that the greater the thickness of the sheet, the better results are obtained, coinciding with what is reported by the manufacturer. On the contrary, in the values of tensile elongation at break (A50) and strain hardening exponent (n), it is observed that the lower the thickness of the sheet, the better results are obtained. These results indicate that the sheet of 20-gauge will have better behavior in drawing operations.

Contrary to what was observed in the metallographic study, a slight anisotropic behavior was presented in the measured mechanical properties, except for the elastic limit. The tensile strength and the hardening coefficient are higher in the samples with an orientation of  $0^\circ$  (in the rolling direction). At the same time, the elongation is lower than in the other two orientations.

Finally, the planar anisotropy values show, for the three thicknesses, a deviation from the optimal value of zero, which indicates a particular susceptibility to the formation of ears in the drawing process.

### Acknowledgment

The authors acknowledge the financial support of the Universidad Nacional Abierta y a Distancia, UNAD, and the Universidad Francisco de Paula Santander, UFPS.

### Reference

- [1] ASM International, *Metals handbook volume 14 forming and forging*. USA: ASM International, 1996.
- [2] J.E. Barbosa, I.H. García, J. Fuentes, “Estimación vía experimental de la formalidad de láminas de aluminio de pureza comercial”, *Rev. Latinoamericana de Metalurgia y Materiales*, vol. 29, no. 2, pp. 128-134, 2009. [Online]. Available: [http://ve.scielo.org/scielo.php?script=sci\\_arttext&pid=S0255-69522009000200008&lng=es&tlng=es](http://ve.scielo.org/scielo.php?script=sci_arttext&pid=S0255-69522009000200008&lng=es&tlng=es)
- [3] C. L. Casadiego, J. E. Barbosa, I. H. García, “Determinación experimental de la formabilidad de láminas de acero SG295 mediante sus propiedades tensiles,” *Rev. colombiana de tecnologías de avanzada*, vol. 1, no. 29, pp. 9-15, 2017, doi: <https://doi.org/10.24054/16927257.v29.n29.2017.2480>
- [4] D.R. Askeland, W.J. Wright, *Ciencia e ingeniería de los materiales*. México, D. F: Cengage learning, 2017.
- [5] R. Gedney, “Sheet Metal Testing Guide”, ADMET, Inc, vol. 1, no. 1, pp. 1-9, 2013, [Online]. Available: <http://admet.com/assets/ADMET-Sheet-Metal-Testing-Guide-July-2013.pdf>
- [6] Standard Test Methods for Tension Testing of Metallic Materials, ASTM E8 / E8M, 2013.
- [7] R. Andersson, “Deformation characteristics of stainless steels,” PhD dissertation, Luleå tekniska universitet, Luleå, 2005, [Online]. Available: <https://www.diva-portal.org/smash/record.jsf?pid=diva2%3A990918&dsid=-4133>
- [8] Standard Test Method for Determining Forming Limit Curves, ASTM E2218, 2015.
- [9] J.A. Newel. *Ciencia de materiales, aplicaciones en ingeniería*. México, D.F: Alfaomega, 2010.
- [10] J.A. Schey. *Introduction to manufacturing processes*. United States Of America: McGraw-Hill, 2000.
- [11] S. Kalpakjian y S.R. Schmid. *Manufactura, Ingeniería y tecnología*. México, D.F: Pearson Educación, 2008.
- [12] Standard Test Method for Plastic Strain Ratio r for Sheet Metal, ASTM E517, 2018.
- [13] A. Güemes, N. Martín, *Ciencia de materiales para ingenieros*. México, D.F: Pearson Educación, 2013.
- [14] Standard Test Method for Tensile Strain-Hardening Exponents (n -Values) of Metallic Sheet Materials, ASTM E646, 2016.
- [15] N.E Dowling. *Mechanical Behavior of Materials*. England: Pearson Education Limited, 2013.
- [16] A. E. Tekkaya, T. Altan. *Sheet Metal Forming: Fundamentals*. USA: ASM International, 2012.
- [17] C. Doerr, J.Y. Kim, P. Singh, J. Wall, L.J. Jacobs, “Evaluation of Sensitization in Stainless Steel 304 and 304L using Nonlinear Rayleigh Waves”, *NDT and E International*, vol. 88, pp. 17-23, 2017, doi: <http://dx.doi.org/10.1016/j.ndteint.2017.02.007>

[18] M. A. Martínez, J. Ordieres, J. Botella, R. Sánchez, R. Parra, “Influencia del tamaño del grano en las propiedades mecánicas de los aceros inoxidables austeníticos”, *revmetal*, vol. 41, no. Extra, pp. 64–68, 2005, doi:

<https://doi.org/10.3989/revmetalm.2005.v41.iExtra.1000>

[19] J. Coello, V. Miguel, A. Calatayud, A. Martínez, C. Ferrer, “Deformability analysis of the AISI 304 DDQ stainless steel under deep drawing multiaxial condition. Evaluation of the initial strain influence”, *Revista de Metalurgia*, vol. 46, no. 5, pp. 435–445, 2010, doi:

<http://dx.doi.org/10.3989/revmetalm.0967>

[20] M. Toit, H. Steyn, “Comparing the Formability of AISI 304 and AISI 202 Stainless Steels”, *Journal of Materials Engineering & Performance*, vol. 21, no. 7, pp. 1491–1495, 2012, doi:

<https://doi.org/10.1007/s11665-011-0044-8>

[21] V. Talyan, R.H. Wagoner, J.K. Lee, “Formability of Stainless Steel”, *Metallurgical and Materials Transactions*, Vol. 29, no. 3, pp. 2161–2172, 1998. doi:

<https://doi.org/10.1007/s11661-998-0041-1>

[22] Standard Specification for Chromium and Chromium-Nickel Stainless Steel Plate, Sheet, and Strip for Pressure Vessels and for General Applications, ASTM A240 / A240M, 2020.

[23] M. J. Serenelli, M. A. Bertinetti, J. W. Signorelli, “Influencia de la textura cristalográfica en la dispersión de coeficientes de lankford en una chapa de acero galvanizada de bajo carbono”, *Mecánica Computacional*, vol XXVII, pp. 993- 1001, 2008. [Online]. Available:

<https://cimec.org.ar/ojs/index.php/mc/article/view/1467>